Available online at www.sciencedirect.com

SciVerse ScienceDirect

Journal of the European Ceramic Society 32 (2012) 835–842

www.elsevier.com/locate/jeurceramsoc

Effect of ethylene glycol on the mullite crystallization

T.M.B. Campos [a], L.S. Cividanes [a,*], D.D. Brunelli [a], K.K. Sakane [b], G.P. Thim [a]

[a] Divisão de Ciências Fundamentais, Instituto Tecnológico de Aeronáutica, Praça Mal. Eduardo Gomes, 50 Vila das Acácias, São José dos Campos, SP, Brazil
[b] Instituto de Pesquisa e Desenvolvimento, Universidade do Vale do Paraíba, Av. Shishima Hitumi, 2911, Urbanova, São José dos Campos, SP, Brazil

Received 18 May 2011; received in revised form 19 September 2011; accepted 30 September 2011
Available online 6 November 2011

Abstract

Mullite is one of the most important aluminosilicate due to its unique thermal properties. In this work, mullite was obtained by sol–gel process at low temperature using sodium metasilicate, water, aluminum nitrate and ethylene glycol. The samples were prepared with a volume ratio of ethylene glycol/water equal to 0/1, 1/1, 2/1 and 3/1. The ethylene glycol effect on mullite crystallization was studied by X-ray diffraction (XRD), Fourier transform-infrared spectroscopy (FT-IR), Scanning Electron Microscopy (SEM) and Differential Thermal Analysis (DTA). The sample prepared without ethylene glycol, the less homogeneous one, formed amorphous silica, spinel-phase and α-alumina at 1000 °C, and then crystallized mullite at 1200 °C, with an alumina molar fraction of 0.58. The other samples formed amorphous silica at 900 °C and crystallized mullite as the only crystalline phase at 1000 °C. However, the alumina content in mullite formula depends on the thermal treatment, reaching 0.58 at 1250 °C.

Keywords: Mullite; Crystallization; Ethylene glycol

1. Introduction

High-purity aluminosilicate with mullite bulk composition is an interesting material to be used in optical[1] and electrical[2] components, separation and purification membranes,[1] porous coatings[1] and biological processes.[3,4] Mullite shows excellent heat resistance, high strength and high creep resistance at both low and high temperatures, heat strike resistance, low thermal expansion coefficient, chemical stability and high temperature strength.[5–11]

Mullite is the only stable compound in the SiO_2–Al_2O_3 system under ambient condition.[12,13] It crystallizes with the following structural formula: $Al_2[Al_{2+2x}Si_{2-2x}]O_{10-x}$, where x is related to the number of oxygen vacancies in the mullite formula.[14] The thermodynamically stable mullite shows x values from 0.25 to 0.40, corresponding to the alumina molar fraction of 0.60 and 0.67, respectively. These composition limits are related to $3Al_2O_3{\cdot}2SiO_2$ and $2Al_2O_3{\cdot}SiO_2$, respectively.[15] Nevertheless, the values out of this range refer to metastable compounds.

Mullite synthesis by sol–gel process is one of the most attractive research fields due to its capacity of producing highly pure ceramic at lower temperature.[16] Therefore, a massive number of works has been done about the processing and characterization of the materials, with mullite composition, derived from the sol–gel process.[17] However, depending on the starting materials and the sol–gel method, the precursors have different properties, what in turn affects the resulting properties of the ceramics.[18] In general, the performance of mullite is remarkably dependent on its microstructure, which is, on the other hand, dependent on the homogeneity of the precursors that lead to crystallization. Therefore, one of the most attractive activities of this research field is to obtain precursors of mullite with high level of homogeneity. The homogeneity of the mullite precursor is often evaluated by the crystallization temperature and the presence of phases different from mullite during the crystallization path. The classification of precursors depends on their homogeneity level, and they are often divided into three types. The most homogeneous one crystallizes mullite at about 1000 °C, and the content of alumina is the same of the precursor bulk.[19–22] The less homogeneous is formed due to differences in the kinetics of hydrolysis and low stability of the sun. It can induce heterogeneous regions within the gel,[23,24] leading to the formation of an intermediate phase (spinel-phase or alumina) at ∼1000 °C and mullite is

* Corresponding author.
E-mail address: lu_civi@yahoo.com.br (L.S. Cividanes).

0955-2219/$ – see front matter © 2011 Elsevier Ltd. All rights reserved.
doi:10.1016/j.jeurceramsoc.2011.09.028

crystallized at temperatures higher than 1200 °C with alumina content equal the precursor.[25] The last kind of precursor has homogeneity between the two first ones and leads to a crystallization of mullite with alumina content different from the starting content at about 1000 °C, together with spinel-phase. The mullite obtained from the third kind of precursor leads to a metastable phase, in which the alumina content is higher than the stable one. The fraction molar of alumina present in the mullite prepared under this condition is generally about 0.77 ($x = 0.61$). The crystalline structure of this metastable mullite is singular, since the cell parameters a and b are equal, and this kind of mullite is often called tetragonal or Al-rich mullite. X-ray powder diffraction analysis is able to differentiate mullite with $x = 0.61$ from the others taking into account its peak at 26° (2θ). While mullite with $x = 0.61$ ($a = b$) shows a single peak at 26°, mullite with $x \neq 0.61$ ($a \neq b$) shows a doubled one.[4]

In this work, mullite was crystallized at low temperature using sodium metasilicate as silica source and nitrate aluminum as alumina source by a sol–gel process. In this scope, the sol–gel synthesis was performed in a medium composed of ethylene glycol and water. The effect of the volume ratio of ethylene glycol/water used to prepare the sol was analyzed by means of DTA, XRD, FT-IR and SEM.

2. Experimental

Silica sol was obtained by passing an aqueous sodium metasilicate (Vetec, Brazil) solution through a cationic exchange resin (IR120, Dow Corning). The silica content was determined by titration and water was added to it for adjusting the silica content to 0.5 mol/L. Four equal samples of this suspension were separated, and ethylene glycol (Vetec, Brazil) was added to them in order to obtain solutions with the following ethylene glycol/water volumetric ratio: 0, 1, 2 and 3, respectively. Aluminum nitrate nonahydrate (Reagen, Brazil) was added to each sample, maintaining the aluminum/silicon molar ratio of 3/1. The samples with ethylene glycol/water volumetric ratio equal to 0, 1, 2 and 3 were denominated SP-0, SP-1, SP-2 and SP-3, respectively. All samples were put into opened vessels and maintained in the oven (80 °C) until xerogel formation.

The xerogels SP-0, SP-1, SP-2 and SP-3 were fired at 450 °C for 2 h and the resulting powder was analyzed through differential thermal analysis (NETZSCH STA 449C) at a heating rate of 15 °C/min and under a flux of 100 mL/min of the oxygen/nitrogen (20%/80%) atmosphere. The 450 °C fired samples were calcined at 900, 1000, 1100, 1200 and 1250 °C for 5 h and the resulting powder was analyzed by X-ray diffraction in a Philips model PW 1830/1840 equipment, using CuKα radiation, and FT-IR equipment (Spot Light 400 Perkin Elmer) using KBr pellet. CaF_2 (with approximately the same mass) was introduced into the fired samples. The XRD intensities at 26 (related to mullite) and 28° (2θ) (related to CaF_2) were determined. The relative yield of mullite crystallization process was determined by the following relation:

$$\text{Relative yeild} = \frac{I_{26}}{I_{28}} \times 100$$

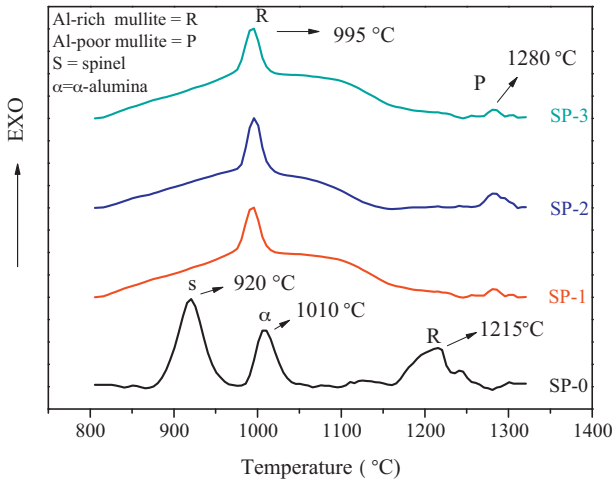

Fig. 1. DTA curve from 800 to 1350 °C of samples SP-0, SP-1, SP-2 and SP-3.

where, I_{26} stands for the intensity of the XRD profile at 26 (2θ) divided by the mass of the fired sample; and I_{28} stands for the intensity of the same XRD profile at 28 (2θ) divided by the mass of CaF_2 introduced into the fired sample. Xerogels calcined at 900 °C for 5 h were pressed, polished and analyzed by SEM in a Jeol model JSM 5310 equipment with energy dispersive X-ray (EDX-elemental mapping).

Mullite can be described by the following formula $Al(VI)_2[(Al(IV)_{2+2x}Si(IV)_{2-2x})]O_{10-x}$. Ruscher and coworkers[24] showed a plot of the values of "x" versus I_{1130}/I_{1170}. Where, I_{1130} and I_{1170} stand for the intensity of the FT-IR bands around 1130 and 1170 cm^{-1}, respectively. By a linear fitting procedure, one can determine that Rüscher's data can be expressed by: $\frac{I_{1130}}{I_{1170}} = (0.56 \pm 0.04) + (1.2 \pm 0.1) * x$. Therefore, once the value of I_{1130}/I_{1170} of a particular FT-IR spectrum is determined, the value of "x" related to that sample can be determined by the previous equation.

3. Results and discussion

Fig. 1 shows the DTA traces of milled samples pre-treated at 450 °C for 2 h. DTA curves of samples SP-1, SP-2 and SP-3 are very similar and they are basically constituted of 2 exothermic peaks: the first one at 995 °C and the second at 1230 °C. However, the DTA profile related to sample SP-0 is quite different from those related to the other samples, showing the presence of at least 3 exothermic events: 920, 1010 and 1215 °C. The XRD profiles of each sample, previously treated at 900, 1000, 1100, 1200 and 1250 °C for 5 h, were also obtained in order to correlate the crystalline phases with the thermal events observed in the DTA analysis.

Fig. 2A and B shows the XRD profiles of samples treated at 900 °C and 1000 °C, respectively. Fig. 2A shows no crystalline peaks in the XRD profiles of samples SP-1, SP-2 and SP-3, while the presence of peaks related to spinel-phase can be observed in the XRD profile of sample SP-0. Fig. 2A also shows broad bands at around 25° (2θ) which are related to the presence of amorphous silica. Fig. 2B shows that the sample SP-0 fired at 1000 °C crystallizes the spinel-phase and α-alumina

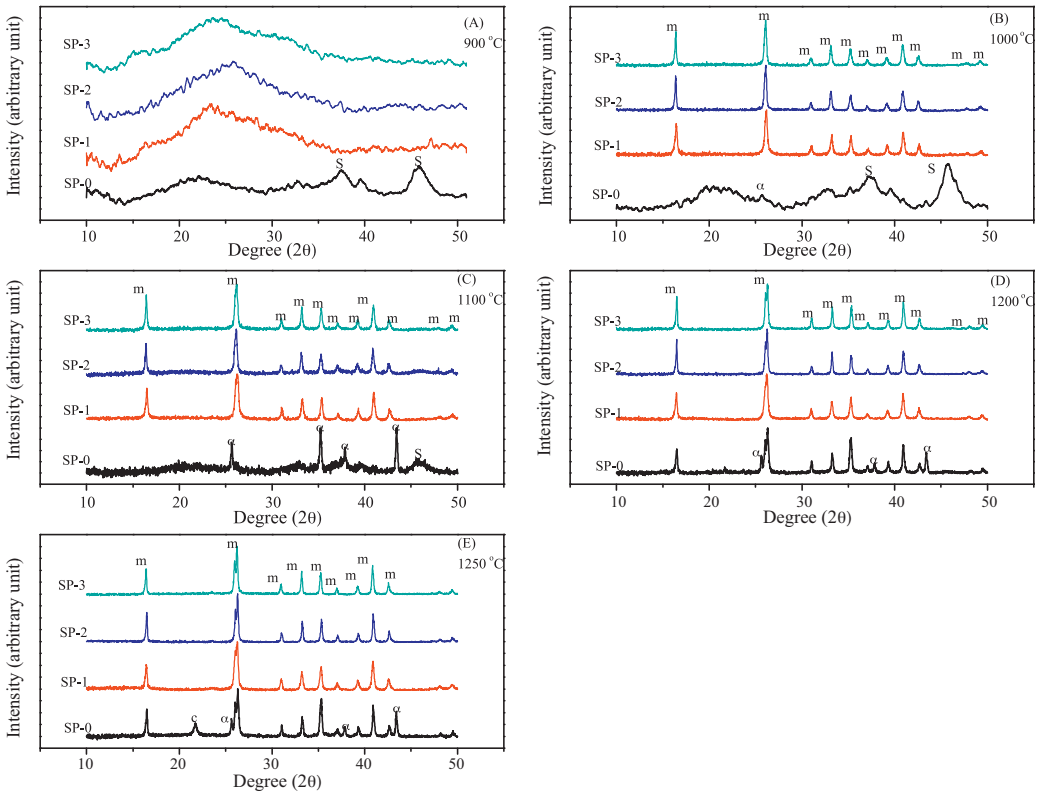

Fig. 2. XRD profiles of samples SP-0, SP-1, SP-2 and SP-3. (A) Samples treated at 900 °C, (B) 1000 °C, (C) 1100 °C, (D) 1200 °C and (E) 1250 °C.

phases (JCPDS 10-173), while the samples SP-1, SP-2 and SP-3 fired at same temperature crystallized only mullite (JCPDS: 15-0776). Therefore, the thermal event observed at the DTA analysis of sample SP-0 at 920 °C may be related to the spinel-phase crystallization and the thermal event at 1010 °C is associated to α-alumina crystallization. The thermal event at 995 °C observed in the DTA analysis of samples SP-1, SP-2 and SP3 is related to mullite crystallization (Table 1).

Fig. 3A shows the FT-IR spectra of samples SP-0, SP-1, SP-2 and SP-3 fired at 900 °C for 5 h. One can observe that the intensity of band J, related to stretching bonding of Al–O_4, and band O, related to stretching bonding of Al–O_4 or Al–O_5, increases when the content of ethylene glycol also increases. However, one can also observe that the intensity of band D, related to the presence of the Al–O_6 stretching, is very strong in the sample SP-0 and very weak in samples SP-1, SP-2 and SP-3. Therefore, the fact that samples SP-1, SP-2 and SP-3 lead to the crystallization of mullite at 1000 °C without going through spinel-phase or α-alumina, may be related to the presence of chemical species formed by Al(IV) and Al(V) in the samples fired at 900 °C, while the presence of spinel-phase and alumina in sample SP-0 calcinated at 1000 °C should be associated to a higher content of Al(VI).

The band associated with label A is related to Si–O–Si bend bonding, indicating that all samples led to silica formation. However, the relative intensity of this band in the FT-IR of sample SP-0 is much stronger than the others. Therefore, one can expect the silica presence in all samples treated at 900 °C, but the

Table 1
Assignment of bands of FT-IR transmittance in the region of 400–1350 cm^{-1} for samples SP-0, SP-1, SP-2 and SP-3. T = Si or Al.

Wavenumber (cm^{-1})	Bonding	Label	Refs.
1220	Si–O–Si (aluminosilicate) ν	M	4,26,27
1170	Si–O–Si or AlO_4 (aluminosilicate) ν	J	4,26,27
1130	Si–O–Si (aluminosilicate) ν	I	4,26,27
1100	Si–O–Si (SiO_2) ν	L	4,26,27
970–1080	Si–O–T (AlO_4 or SiO_2) ν	H	4,26,27
808–883	Al–O (AlO_4) ν	G	4,26,27
825	Al–O (AlO_4) ν	F	4,26,27
742–749	T–O–T (TO_4) ν (T = Si or Al)	E	4,26,27
650	Al–O (AlO_5) ν	O	4,26,27
548–578	Al–O–T or Al–O–Al(AlO_6) ν	D	4,26,27
570	Si–O–Si ν	C	4,26,27
482–498	Si–O–Si bend	A and B	4,26,27

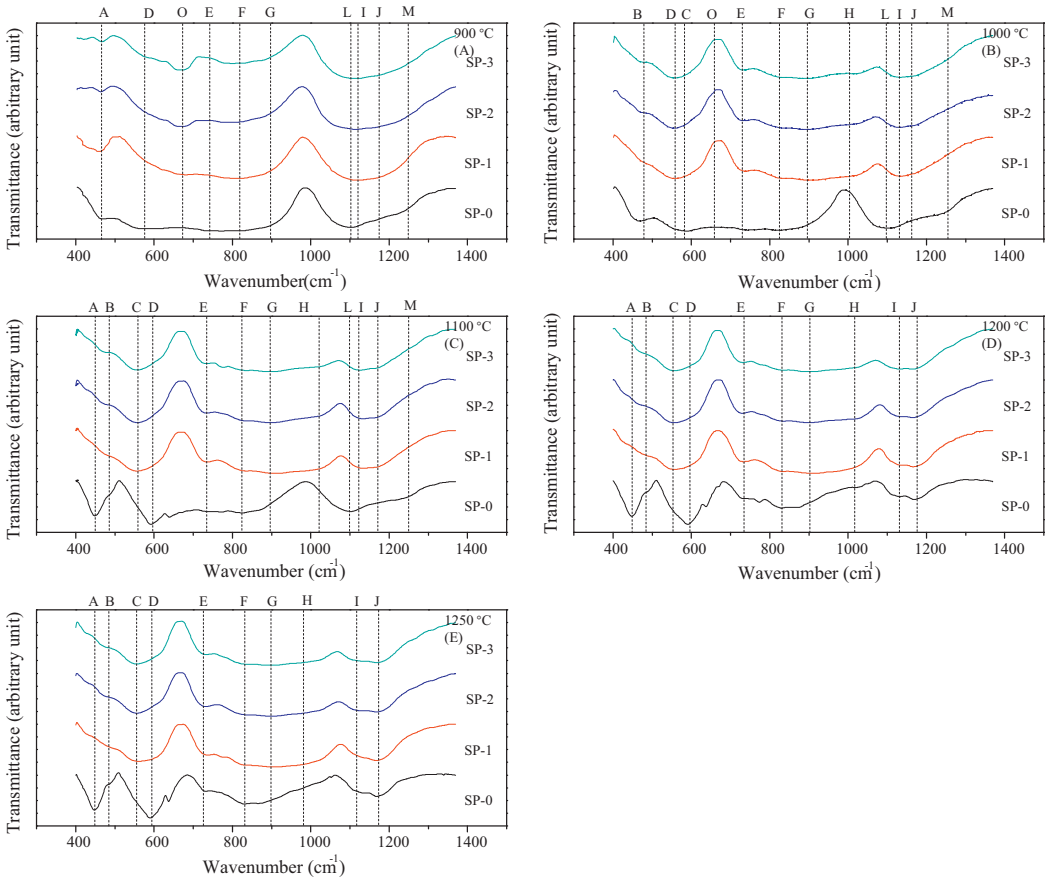

Fig. 3. FT-IR spectra of samples SP-0, SP-1, SP-2 and SP-3. (A) Treated at 900 °C, (B) 1000 °C, (C) 1100 °C, (D) 1200 °C and (E) 1250 °C. The letters at the top of the figure are described in Table 1.

silica quantity in SP-0 must be much higher than in the others. The peak at around 600 cm^{-1} in the FT-IR spectra is related to Al–O–Al bonding, associated to alumina formation. These results confirm those obtained from XRD analysis, indicating that the sample SP-0 treated at 1000 °C is constituted of a silica and alumina mixture. The sizes of the alumina and silica particles present in the samples can be evaluated by energy dispersive X-ray (EDX-elemental mapping) analysis, which is presented in Fig. 4. Fig. 4A shows SEM images of each sample treated at 900 °C for 5 h. Figs. 4B and 5C are EDX dot map of Image 5A, showing the Al and Si distribution in the image represented in Fig. 4A. The bright area in Fig. 4B is related to aluminum and the one in Fig. 4C is associated to the silicon atom.The white arrows in Fig. 4 are only guides for the eyes. In the images related to sample SP-0, one can see that the images of silicon and aluminum are complementary. A white region in the silicon image corresponds to a dark area in the aluminum images and vice versa. This is an unambiguous indication that this sample is constituted of micrometric particles of silica and alumina. The presence of alumina and silica particles in sample SP-0 confirms the results of FT-IR and XRD. The FT-IR spectra of sample SP-0 showed the presence of bands related to chemical groups of Si–O–Si and Al–O–Al, forming isolated clusters of silica and alumina at 900 °C, while XRD profiles of the same sample showed the presence of alumina and a large band, which is characteristic in amorphous silica. samples SP-1, SP-2 and SP-3 also show the presence of bright areas in Fig. 5B and C, however they are not complementary images. The bright areas in Fig. 4B correspond to the bright areas in Fig. 4C. Therefore, one cannot observe either the presence of micrometric particles of silica or alumina. Therefore, samples SP-1, SP-2 and SP-3 are constituted by silicon and aluminum particles whose sizes are much smaller than those present in sample SP-0.

Fig. 3B shows the FT-IR spectra of samples SP-0, SP-1, SP-2 and SP-3 calcined at 1000 °C for 5 h. The band O, related to Al–O_5 chemical species, is not present in the FT-IR spectra of samples SP-1, SP-2 and SP-3. However, one can observe the presence of band D, which is related to the chemical species Al(VI). In these samples, the mullite crystallization process occurred by the consumption of Al(V), changing them to more stable one Al(VI), which is present in the mullite crystalline structure. Mullite crystallization depends on the distance between aluminum and silicon atoms present in the xerogels, since the chemical bonding Al–O–Si must be formed during the crystallization process.[28] The silicon atom is always tetracoordinated, but aluminum can be found in the xerogels as tetracoordinated [Al(IV)], pentacoordinated [Al(V)] or hexacoordinated [Al(VI)]. There is an agreement in literature that aluminum coordination at about 1000 °C plays a fundamental role in the mullite crystallization mechanism.[30] Jaymes and

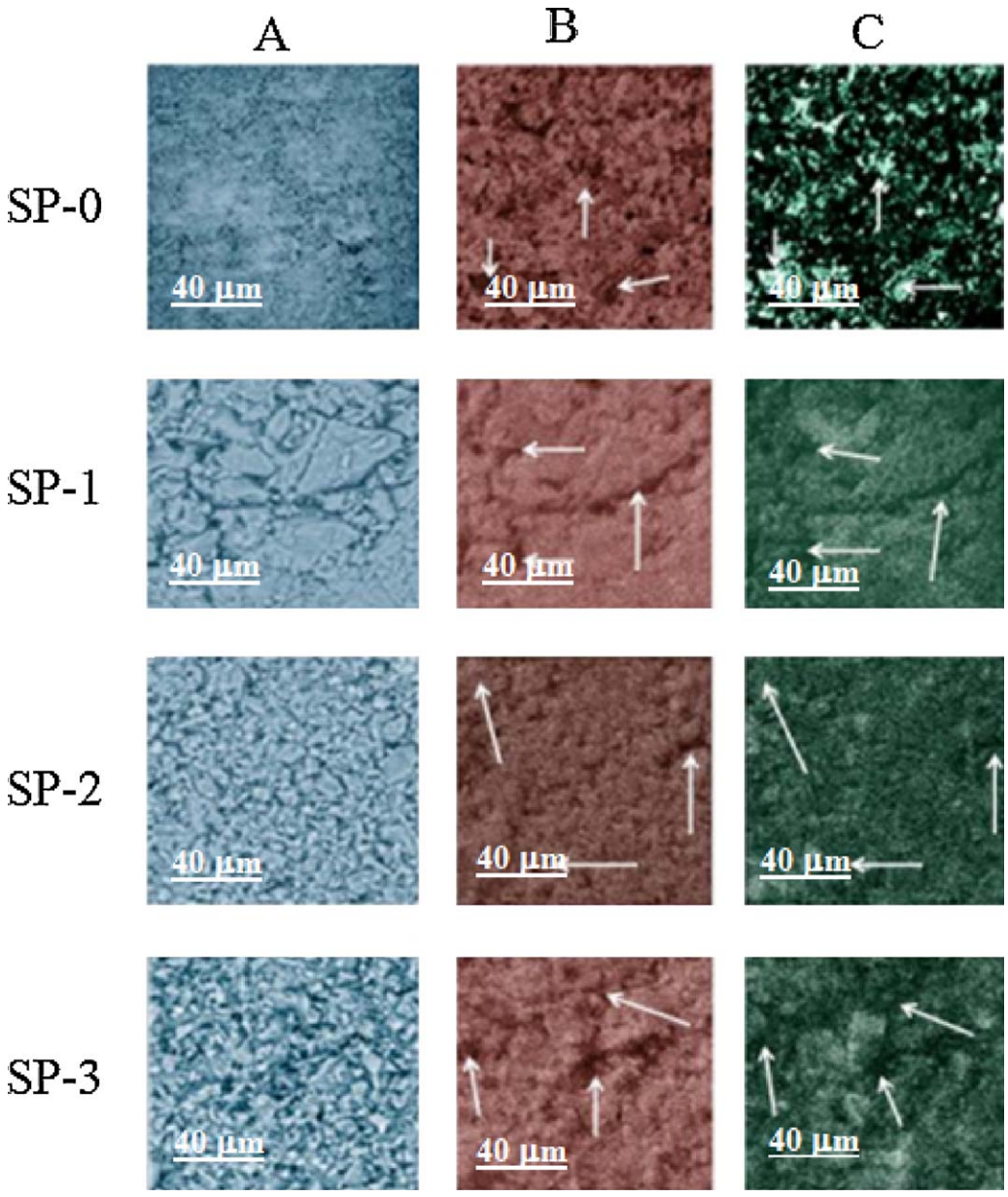

Fig. 4. SEM-EDX of all samples treated at 900 °C. SEM-EDX dot map showing Al (B) and Si (C) distribution of the image represented in SEM images (A).

co-workers observed that highly homogeneous xerogels showed high contents of Al(IV) and Al(V) at about 900 °C and they observed mullite crystallization at 1000 °C,[28,29] while Gerardin and co-workers observed that the less homogenous xerogels had higher contents of Al(VI), crystallizing spinel-phase at 1000 °C and mullite at 1200 °C.[30] Okuno and co-workers[31] associated the observations of Jaymes and Gerardin to the difference in stability of the coordinated aluminum, i.e. Al(VI) is a much more reactive chemical species into a silica medium at around 1000 °C than Al(IV) and Al(V) chemical species.[4] Okuno and co-workers[31] also observed that species Al(V) is not stable at temperatures higher than 900 °C.

Mullite can be represented by the formula $Al(VI)_2[(Al(IV)_{2+2x}Si(IV)_{2-2x})]O_{10-x}$. The value of x is associated with the replacement of Si(IV) by Al(IV) in the tetrahedral sites, generating oxygen holes. Its value depends on molar concentration of alumina (Al_2O_3) in the mullite formula, according[24] to Eq. (1).

$$x = 10 - 6\left[\frac{m + 200}{m + 100}\right] \quad (1)$$

where, m is the molar percentage of alumina.

Mullite is in fact a solid solution and it is thermodynamically stable when its composition varies between $x = 0.25$ and $x = 0.40$. Mullite with a $3Al_2O_3{\cdot}2SiO_2$ composition corresponds to $x = 0.25$ and the molar fraction of alumina is 0.60, while mullite with a $2Al_2O_3{\cdot}SiO_2$ composition corresponds to $x = 0.40$ and the alumina molar fraction is equal to 0.67.[24] The percentage of Al_2O_3 present in mullite structure in samples SP-0, SP-1, SP-2 and SP-3 after the burning steps at 900, 1000, 1100, 1200 and 1250 °C was determined using this FT-IR technique.

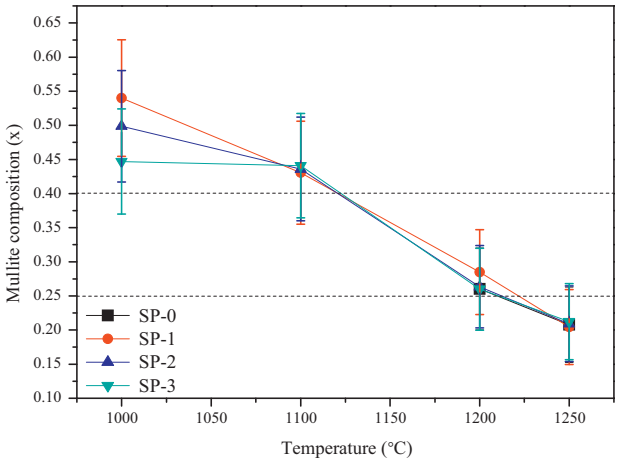

Fig. 5. Dependence of mullite composition with temperature of thermal treatment.

The peaks at 1130 and 1170 cm^{-1} are related to the presence of mullite, therefore, FT-IR experiments confirmed what Fig. 2B has already showed: sample SP-0 did not crystallize mullite during firing step at 1000 °C, while SP-1, SP-2 and SP-3 did. No value of x was attributed in relation to sample SP-0, but values of x equal to 0.54, 0.49 and 0.45 were determined for samples SP-1, SP-2 and SP-3 treated at 1000 °C, which correspond to alumina molar fraction of 0.73, 071 and 0.69 respectively.

Fig. 2C shows the XRD profiles of samples treated at 1100 °C for 5 h. No change is observed in the XRD profiles of SP-1, SP-2 and SP-3 samples fired at 1100 °C in relation to those fired at 1000 °C, but a remarkable change can be observed in the profile of sample SP-0 fired at 1100 °C. The XRD profile of sample SP-0 fired at 1100 °C shows well defined peaks of α-alumina and these peaks are much more intense than those related to spinel-phase. Therefore, one can confirm that those thermal events at 1010 °C must be related to α-alumina crystallization, since this sample certainly crystallized spinel-phase before α-alumina.

The FT-IR spectra of samples SP-1, SP-2 and SP-3 treated at 1100 °C for 5 h are showed in Fig. 3C. The band about 400 cm^{-1} (band A) is a characteristic of the Si–O–Si chemical bonding related to silica formation. However, the XRD profile showed in Fig. 2C did not show the presence of peaks associated to any form of crystalline silica, indicating the presence of the amorphous silica. The band about 600 cm^{-1} (C and D) is related to the Al–O–Al chemical bonding and the XRD profile showed the formation of crystalline alumina in sample SP-0 treated at 1100 °C. This is clear indication that silica and alumina are formed in separated regions of the sample, what may affect the kinetic of mullite crystallization. The x values found in samples SP-1, SP-2 and SP-3 are 0.43, 0.44 and 0.44, respectively, which correspond to alumina molar fractions of 0.68, 0.69 and 0.69. Considering the experimental error, all of them have the same value. The decrease in the x values in the samples treated at 1100 °C in relation to those treated at 1000 °C means that samples treated at 1100 °C are richer in silica than those samples treated at 1000 °C, similar results were obtained by Ruscher and co-workers[24] during mullite crystallization from highly homogenous precursors.

Fig. 2C shows XRD profiles of samples treated at 1200 °C. There is only one difference between XRD of samples treated at 1100 and 1200 °C: the XRD profiles of sample SP-0 showed the presence of mullite. Mullite is formed at 1200 °C in sample SP-0 because the diffusion rate of silica in alumina is much higher at this temperature than at 1100 °C.[32] Therefore, mullite was formed in the sample without ethylene glycol at a temperature 200 °C higher than that in which mullite is formed from xerogels prepared with ethylene glycol. This huge temperature difference and the mullite crystallization at 1000 °C are significant properties for the synthesis of mullite based on an aqueous silicon source, which was provided in this work by the metasilicate salt. As far as we know, these properties were obtained only when TEOS (tetraethyl orthosilicate) was used as silicon source and the procedure was performed in alcohol medium.

The FT-IR spectra of samples SP-1, SP-2 and SP-3 showed in Fig. 3D are quite similar, the only difference is in relation to the relative intensity of peaks at 1170 and 1130 cm^{-1}. FT-IR of sample SP-0 shows bands G, H, I and J that are characteristics of aluminosilicates. The band about 400 cm^{-1} is a characteristic of the Si–O–Si chemical bonding and it is related to silica formation. However, XRD profile showed in Fig. 2D did not show the presence of peaks associated to any form of crystalline silica, indicating that the silica present in sample SP-0 was in the amorphous phase. The band about 600 cm^{-1} (bands C and D) is related to Al–O–Al chemical bonding and XRD profile showed the formation of crystalline alumina.

The values of "x" in the mullite formula obtained by firing samples SP-0, SP-1, SP-2 and SP-3 at 1200 for 5 h are equal to 0.26, 0.28, 026 and 0.26, corresponding to alumina molar fraction of 0.58, 0.61, 0.60 and 0.60, respectively. Among all samples, SP-0 crystallized mullite at higher temperature but this sample leads to mullite crystallization with the formula $3Al_2O_3{\cdot}2SiO_2$, which has aluminum/silicon ratio equal to the composition of starting materials. The fact that less homogenous materials crystallized mullite with the composition equal to bulk composition, can be explained by the diffusion process of alumina into silica, making the silica particle richer in alumina with the increase of the thermal treatment time.

Fig. 2E shows the XRD profiles of samples SP-0, SP-1, SP-2 and SP-3 treated at 1250 °C for 5 h. XRD profiles related to sample SP-1, SP-2 and SP-3 show basically the same peaks and intensity of those showed in Fig. 2D. However, in this Figure one can see shoulders on the left side of the peak at 26° (2θ). In fact, these shoulders were already present in the previous XRD profiles of these samples, but they have approximately the same intensities and were very close to one another, making it difficult to identify the presence of two peaks. The XRD profiles of sample SP-0 fired at 1250 °C is quite different from that one related to the same sample fired at 1200 °C. Fig. 2E shows the presence of peaks of mullite together with alumina and cristobalite peaks, performing a complete phase separation.

Fig. 3E shows FT-IR spectra of samples SP-0, SP-1, SP-2 and SP-3 calcined at 1250 °C for 5 h. There are no significant changes in relation to those showed in Fig. 3D, related to the samples fired at 1200 °C, since those samples calcined at 1250 °C have the same chemical composition that those fired at 1200 °C. The

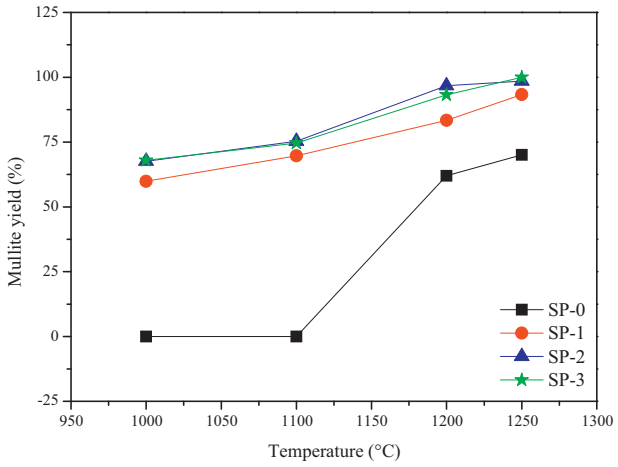

Fig. 6. Relative yield of mullite crystallization from SP-0, SP-1, SP-2 and SP-3 with firing temperature.

x values and alumina molar fractions of SP-0, SP-1, SP-2 and SP-3 are, respectively: x values = 0.21, 0.20, 0.21 and 0.21 and molar fractions = 0.58, 0.58, 0.58 and 0.58.

Fig. 5 shows a plot of x with thermal treatment. The dotted line in the plot indicates the stable limit of mullite composition, ranging from molar fraction of alumina of 0.60; $x = 0.25$ ($3Al_2O_3{\cdot}2SiO_2$) to fraction molar of 0.67; 0.40; ($2Al_2O_3{\cdot}SiO_2$).[24] Mullite did not crystallize in sample SP-0 treated at 1000 and 1100 °C, therefore there are no x values for this sample in these temperatures. The x values and alumina molar fraction decreased with the increase of temperature of thermal treatment independent on the kind of sample. Considering the average values, x in all samples at 1100, 1200 and 1250 are very close. Actually, these experimental points are superimposed in the plot. The average values for 1000 °C are quite different, but taking the error bars into account one can consider that they are the same. This analysis indicates that alumina composition in mullite and consequently oxygen vacancies are dependent only on temperature. However, the extension of the alumina + silica → mullite transformation is dependent on the kind of precursor.[33,34] Fig. 6 shows the relative yield of mullite crystallization at several firing temperatures, where all values were normalized by the highest one (sample SP-3 at 1250 °C). Mullite crystallization process from sample SP-0 is "late" in relation to the others. Mullite crystallizes from samples SP-1, SP-2 and SP-3 at 1000 °C, however, from sample SP-0 it started at 1200 °C. Nevertheless, a remarkable fact is the difference in the relative yield between samples ethylene glycol processed. Sample SP-1 always shows a relative yield about 5% lower in relation to the others during all thermal processing. However, Fig. 6 also shows that there is no difference in the yield of mullite crystallization from SP-2 to SP-3. Therefore, one can conclude that ethylene glycol influences the kinetic process of mullite crystallization, but systems with ethylene glycol concentration higher than a limit value seems not to influence the process.

The gel time of suspensions prepared with silicic acid, EG and water was very dependent on EG contents. Suspensions without ethylene glycol gelled in 02 days, while that one with proportions of sample SP-3 (opened at 80 °C) forms gel in approximately 10 days. Silanol in water quickly form gels through condensation process of monomers, dimers or trimmers. However, the dissolution of aluminum salt in water forms the aquo complex $[Al(H_2O)_6]^{3+}$, which is very stable and do not form gels. Therefore, solutions constituted of silicic acid, aluminum nitrate and water form silica gels and the aluminum ions are dissolved, as $[Al(H_2O)_6]^{3+}$, in the water that permeates silica particles. The aluminum ions cannot be homogenously distributed in the entire gel due to silica particle formation.

Solutions (opened at 80 °C) prepared with aluminum ions, ethylene glycol and water often form tridimensional gels (like silica gels) and the gel time is also dependent on the ethylene glycol concentration. Samples SP-1, SP-2 and SP-3 are constituted of silicic acid, aluminum nitrate, water and ethylene glycol. The ethylene glycol content used in these samples was chosen in order to hold the gel time of silica and alumina approximately the same. Therefore, the gel formed from these samples can be constituted of two mixed gels (silica and alumina) or only one gel.

Mizukami and co-workers[35] obtained mullite from tetraethoxyorthosilicate (TEOS), aluminum nitrate, ethylene glycol and water. They correlated the influence of EG on the mullite crystallization path to the presence of diols chemical group in the EG molecule. This group was considered able to connect both the aluminum and silicon atoms, suggesting the existence of the Al–OCH_2CH_2O–Si structure.

Yabuki and co-workers[36] also prepared gels from TEOS, aluminum nitrate, EG and water. The as-dried gels were characterized by[27] ALMASNMR Al (magic-angle-spinning). They observed the presence of peaks related to 4-coordinated, 5-coordinated and 6-coordinated aluminum and suggested the formation of a structure similar to that one proposed by Mizukami and co-workers (Al–OCH_2CH_2O–Si). They observed the presence of 5-coordinated and 6-coordinated aluminum even in the sample dried at 50 °C, and the relative proportion of 4-coordinated and 5-coordinated in relation to 6-coordinated aluminum increased with temperature. The 4-coordinated and 5-coordinated species were in greater number in samples treated at 300 °C.

The presence of 4 and 5-coordinated aluminum in samples SP-1, SP-2 and SP-3 treated at 900 °C is a strong indication that EG effected the structure of gels. Where, one molecule of ethylene glycol could be connected to aluminum and silicon simultaneously, forming a structure similar to the one initially proposed by Mizukami and co-workers (Al–OCH_2CH_2O–Si). The mullite precursor constituted of such structure has enough homogeneity to crystallize mullite at 1000 °C, as it was observed in this work.

4. Conclusions

Ethylene glycol increases the homogeneity of the samples prepared by the colloidal sol–gel method in an aqueous medium. sample SP-0 treated at 900 °C is composed by big sized particles of alumina and silica, resulting in the spinel-phase formation at 900 °C, α-alumina at 1000 °C and mullite at 1200 °C. However, samples SP-1, SP-2 and SP-3 treated at 900 °C are composed

by very small particles of silica and alumina, resulting in the direct mullite crystallization at 1000 °C. FT-IR results showed that samples SP-1, SP-2 and SP-3 treated at 900 °C are rich in Al(IV) and Al(V) chemical species, but the contents of these species decreased a lot when these samples were treated at 1000 °C, forming mullite. Therefore, Al(IV) and Al(V) contents in samples at temperatures less than 1000 °C can be a decisive factor for crystallizing mullite at 1000 °C. The contents of alumina in the mullite formula do not depend on the precursor, but it depends on temperature. Mullite crystallizes at 1000 °C with alumina molar composition related to a metastable solution and at higher temperatures silica is incorporated to this metastable solid solution, reaching the stable composition. Ethylene glycol influenced the mullite kinetic crystallization and it seems that the relative yield depends on the ethylene glycol contents. However, ethylene glycol does not influence the composition of alumina in the mullite structure.

Acknowledgements

The authors thank Fundação de Amparo à Pesquisa no Estado de São Paulo (FAPESP#2007/02701-5) and Conselho Nacional de Pesquisa (CNPq#552299/2009-0) for financial support.

References

1. Vendange V, Colomban P. How to tailor the porous structure of alumina and aluminosilicate gels and glasses. *J Mater Res* 2011;**11**:518–28.
2. Sinkó K. Transformation of aluminosilicate wet gel to solid state. *J Solid State Chem* 2002;**165**:111–8.
3. Leivo J, Meretoja V, Vippola M, Levänen E, Vallittu P, Mäntylä TA. Sol–gel derived aluminosilicate coatings on alumina as substrate for osteoblasts. *Acta Biomater* 2006;**2**:659–68.
4. Leivo J, Linden M, Rosenholm J, Ritola M, Teixeira C, Levanen E, et al. Evolution of aluminosilicate structure and mullite crystallization from homogeneous nanoparticulate sol–gel precursor with organic additives. *J Eur Ceram Soc* 2008;**28**:1749–62.
5. Kanka B. Aluminosilicate fiber/mullite matrix composites with favorable high-temperature properties. *J Eur Ceram Soc* 2000;**20**:619–23.
6. Kaya C, Butler EG, Selcuk A, Boccaccini AR, Lewis MH. Mullite (Nextel^{TM} 720) fibre-reinforced mullite matrix composites exhibiting favourable thermomechanical properties. *J Eur Ceram Soc* 2002;**22**:2333–42.
7. Dlouhy I, Chlup Z, Boccaccini DN, Atiq S, Boccaccini AR. Fracture behaviour of hybrid glass matrix composites: thermal ageing effects. *Compos Part A: Appl S* 2003;**34**:1177–85.
8. Delegrlise F. Microstructural evolution under load and high temperature deformation mechanisms of a mullite/alumina fibre. *J Eur Ceram Soc* 2002;**22**:1501–12.
9. Kriven W. High temperature single crystal properties of mullite. *J Eur Ceram Soc* 1999;**19**:2529–41.
10. Mileiko S, Serebryakov A, Kiiko V, Kolchin A, Kurlov V, Novokhatskaya N. Single crystalline mullite fibres obtained by the internal crystallisation method: microstructure and creep resistance. *J Eur Ceram Soc* 2009;**29**:337–45.
11. Zhang Y, Ding Y, Gao J, Yang J. Mullite fibres prepared by sol–gel method using polyvinyl butyral. *J Eur Ceram Soc* 2009;**29**:1101–7.
12. Aksay IA, Pask JA. Stable and metastable equilibria in system SiO_2–Al_2O_3. *J Eur Ceram Soc* 1975;**58**:507–12.
13. Klug FJ, Prochazka S, Doremus RH. Alumina–silica phase diagram in the mollite region. *J Am Ceram Soc* 1987;**70**:750–9.
14. Sola ERD, Torres FJ, Alarc J. Thermal evolution and structural study of 2:1 mullite from monophasic gels. *J Eur Ceram Soc* 2006;**26**:2279–84.
15. Rüscher C. Infra-red spectroscopic investigation in the mullite field of composition: $Al_2(Al_{2+2x}Si_{2-2x})O_{10-x}$ with $0.55 > x > 0.25$. *J Eur Ceram Soc* 1996;**16**:169–75.
16. Hench LL, Vasconcelos W. Gel–silica science. *Annu Rev Mater Sci* 1990;**20**:269–98.
17. Chen X, Gu L. The sol–gel transition of mullite spinning solution in relation to the formation of ceramic fibers. *J Sol–Gel Sci Technol* 2008;**46**:23–32.
18. Kurajica S, Tkalcec E, Schmauch J. $CoAl_2O_4$–mullite composites prepared by sol–gel processes. *J Eur Ceram Soc* 2007;**27**:951–8.
19. Huling JC, Messing GL. Chemistry of crystallization relations in molecular mullite gels. *J Non-Cryst Solids* 1992;**147**:213–21.
20. Fischer RX, Schneider H, Voll D. Formation of aluminum rich 9:1 mullite and its transformation to low alumina mullite upon heating. *J Eur Ceram Soc* 1996;**16**:109–13.
21. Ban T, Hayashi S, Yasumori A, Okada K. Characterization of low temperature mullitization. *J Eur Ceram Soc* 1996;**16**:127–32.
22. Bagchi B, Das S, Bhattacharya A, Basu R, Nandy P. Nanocrystalline mullite synthesis at a low temperature: effect of copper ions. *J Eur Ceram Soc* 2009;**92**:748–51.
23. Okada K, Otsuka N. Characterization of the spinel phase from SiO_2–Al_2O_3 xerogels and the formation process of mullite. *J Am Ceram Soc* 1986;**69**(9):652–6.
24. Schneider H, Voll D, Saruhan B, Sanz J, Schrader G, Ruscher C, et al. Synthesis and structural characterization of non-crystalline mullite precursors. *J Non-Cryst Solids* 1994;**178**:262–71.
25. Huling JC, Messing GL. Epitactic nucleation of spinel in aluminosilicate gels and its effect on mullite crystallization. *J Am Ceram Soc* 1991;**74**:2374–81.
26. Okuno M, Zotov N, Schmucker M, Schneider H. Structure of SiO–AlO glasses: combined X-ray diffraction, IR and Raman studies. *J Non-Cryst Solids* 2005;**351**:1032–8.
27. Cividanes LS, Campos TMB, Rodrigues LA, Brunelli DD, Thim GP. Review of mullite synthesis routes by sol–gel method. *J Sol–Gel Sci Technol* 2010;**1**:111–25.
28. Jaymes I, Douy A, Massiot D, Coutures JP. Characterization of mono- and diphasic mullite precursor powders prepared by aqueous routes. 27Al and 29Si MAS–NMR spectroscopy investigations. *J Mater Sci* 1996;**31**:4581–9.
29. Jaymes I. New aqueous mullite precursor synthesis. Structural study by ^{27}Al and ^{29}Si NMR spectroscopy. *J Eur Ceram Soc* 1996;**16**:155–60.
30. Gerardin C, Sundaresan S, Benziger J, Navrotsky A. Structural investigation and energetics of mullite formation from sol–gel precursors. *Chem Mater* 1994;**6**:160–70.
31. Okuno M, Shimada Y, Schmücker M, Schneider H, Hoffbauer W, Jansen M. LAXS and ^{27}Al MAS NMR studies on the temperature-induced changes of non-crystalline single phase type mullite precursors. *J Non-Cryst Solids* 1997;**210**:41–7.
32. Wei W-C, Halloran JW. Transformation kinetics of diphasic aluminosilicate gels. *J Am Ceram Soc* 1988;**71**:581–7.
33. Oliveira TC, Ribeiro CA, Brunelli DD, Rodrigues LA, Thim GP. The kinetic of mullite crystallization: effect of water content. *J Non-Cryst Solids* 2010;**356**:2980–5.
34. Cividanes LS, Campos TMB, Bertran CA, Brunelli DD, Thim GP. Effect of urea on the mullite crystallization. *J Non-Cryst Solids* 2010;**356**:3013–8.
35. Mizukami F, Maeda K, Toba M, Sano T. Effect of organic ligands used in sol–gel process on the formation of mullite. *J Sol–Gel Sci Technol* 1997;**106**:101–6.
36. Yabuki M, Takahashi R, Sato S, Sodesawa T, Ogura K. Silica–alumina catalysts prepared in sol–gel process of TEOS with organic additives. *Phys Chem Phys* 2002;**4**:4830–7.